An Electrochemical Platform for the Carbon Dioxide Capture and Conversion to Syngas

energies

MDPI

Article

An Electrochemical Platform for the Carbon Dioxide Capture and Conversion to Syngas

Alessio Mezza [1,2], Angelo Pettigiani [1,2], Nicolò B. D. Monti [1,2], Sergio Bocchini [1], M. Amin Farkhondehfal [1], Juqin Zeng [1], Angelica Chiodoni [1], Candido F. Pirri [1,2] and Adriano Sacco [1,*]

[1] Center for Sustainable Future Technologies @Polito, Istituto Italiano di Tecnologia, Via Livorno 60, 10144 Torino, Italy; alessio.mezza@polito.it (A.M.); angelo.pettigiani@studenti.polito.it (A.P.); nicolo.monti@iit.it (N.B.D.M.); sergio.bocchini@iit.it (S.B.); amin.farkhondehfal@iit.it (M.A.F.); juqin.zeng@iit.it (J.Z.); angelica.chiodoni@iit.it (A.C.); fabrizio.pirri@iit.it (C.F.P.)

[2] Department of Applied Science and Technology, Politecnico di Torino, Corso Duca degli Abruzzi 24, 10129 Torino, Italy

* Correspondence: adriano.sacco@iit.it; Tel.: +39-011-5091912

Abstract: We report on a simple electrochemical system able to capture gaseous carbon dioxide from a gas mixture and convert it into syngas. The capture/release module is implemented via regeneration of NaOH and acidification of $NaHCO_3$ inside a four-chamber electrochemical flow cell employing Pt foils as catalysts, while the conversion is carried out by a coupled reactor that performs electrochemical reduction of carbon dioxide using ZnO as a catalyst and $KHCO_3$ as an electrolyte. The capture module is optimized such that, powered by a current density of 100 mA/cm^2, from a mixture of the CO_2–N_2 gas stream, a pure and stable CO_2 outlet flow of 4–5 mL/min is obtained. The conversion module is able to convert the carbon dioxide into a mixture of gaseous CO and H_2 (syngas) with a selectivity for the carbon monoxide of 56%. This represents the first all-electrochemical system for carbon dioxide capture and conversion.

Keywords: CO_2 capture; CO_2 conversion; carbon capture and utilization; electrochemical capture; syngas; electrodialysis

Citation: Mezza, A.; Pettigiani, A.; Monti, N.B.D.; Bocchini, S.; Farkhondehfal, M.A.; Zeng, J.; Chiodoni, A.; Pirri, C.F.; Sacco, A. An Electrochemical Platform for the Carbon Dioxide Capture and Conversion to Syngas. *Energies* **2021**, *14*, 7869. https://doi.org/10.3390/en14237869

Academic Editors: Federica Raganati and Paola Ammendola

Received: 3 November 2021
Accepted: 19 November 2021
Published: 24 November 2021

1. Introduction

In the last decades, the problem of the global warming has gained the attention of the research community. To respect the conditions imposed by the Paris Agreement, it is fundamental to keep the carbon emissions as low as possible until the renewable energy sources have substituted the carbon-based fuels.

In this background, carbon capture and storage (CCS) technologies allow the transport of big amount of CO_2 from the point source to safe geological storage, avoiding the release into the atmosphere [1]. However, CCS fails in the productive reusing of the CO_2. On the other hand, the conversion and utilization of the captured CO_2 (CCU), carried out by catalytic reduction to fuel precursors such as syngas [2], is a possibility to achieve a carbon-neutral cycle.

Currently, CO_2 capture using aqueous monoethanolamine (MEA) [3] is the most used one for reducing carbon emission. In several works, the possibility to integrate this process with the catalytic reduction of CO_2 has been investigated [4,5]. Although this process is efficient in terms of capture, it has several drawbacks, the principal one being the high energy amount necessary for the stripping of the CO_2 from the solvent. Bhattacharya et al. showed how it is possible to use carbamate/carbamic acid as substrate for the reduction of carbon dioxide to syngas [6], avoiding the stripping from the amine-based solvent. This could be a good solution for CCU systems in industrial plants, but not for smaller-scale urban applications, since amine-based solvents are highly toxic. Lombardo's work introduced another possibility to integrate capture and reduction of

carbon dioxide to high-end chemicals [7], such as formic acid or N-formylated amine. In this case, ionic liquids (IL) are exploited for fixation and reduction of CO_2, since ILs show excellent CO_2 affinity and have advantageous chemical and physical properties such as high chemical/thermal stability, non-flammability and low vapor pressure [8]. A possible integration between capture and reduction can be done by housing in the same reactor the catalyst and the sorbent [9]. Duyar's dual functional materials [10], composed by a sorbent and a catalyst, allows both capture and conversion (methanation) of CO_2 using H_2 produced by electrolysis. The dual functional materials consist of Ru as methanation catalyst and nano-dispersed CaO as CO_2 adsorbent, both supported on a porous γ-Al_2O_3 carrier. In this way, the capture and utilization occur inside the same reactor operating at a temperature of 320 °C, possibly using heat recovered by the flue gas. Similarly, as Ampelli and coworkers showed, it is possible to implement an electrochemical device including a nanocomposite electrocatalyst based on metal-doped conjugated microporous polymer [11]. Hence, the reduction of carbon comes up directly on the polymer surface that is the responsible for the adsorption of CO_2. Moreover, the tri-reforming of methane allows the carbon conversion and utilization in flue gas without CO_2 separation, producing useful synthesis gas [12]. However, in order to enable the reaction, a source of natural gas in addition to the flue gas is needed.

In this work, a simple new solution for the CCU is proposed, where both the capture and the conversion are performed electrochemically. On one side there is capture from flue gas and releasing of CO_2 via electrodialysis and regeneration of alkaline carbonate solution [13]. On the other side, an electrochemical reactor receiving as inlet pure carbon dioxide, provides syngas as output [14]. This solution, composed by the coupling of two simple electrochemical systems, avoids high temperature and toxic substances, so reducing the energy consumption and making this system a suitable green and low-cost possibility for flue gas conversion.

2. Materials and Methods

2.1. Capture and Release Module

The electrochemical reactor (ElectroCell, Micro Flow Cell) employed for the capture and release of CO_2, whose sketch is depicted in Scheme 1, has a projected electrode area of 0.001 m^2. Two bipolar membranes (FumaTech, fumasep FBM) separate chambers 2 from 4 and 1 from 3, while a proton exchange membrane (Nafion^{TM} Membrane N117, Sigma-Aldrich, St. Louis, MO, USA) separates chambers 3 and 4. This cell employs platinum as a catalyst on both electrodes, 0.8 M sodium bicarbonate ($NaHCO_3$, 99.5%, Sigma-Aldrich) as sorbent solution, and 0.1 M sodium chloride (NaCl, 99.5%, Sigma-Aldrich) as the electrolyte. Each solution has been obtained dissolving the reagents in ultrapure water. A peristaltic pump (Ismatec, MCP) has been used for the recirculation of the solutions inside the chambers of the electrochemical reactor. A constant current has been provided by a source measure unit (Keithley, 2635A), that also performed the voltage acquisitions. Mass flow controllers/meters (Bronkhorst, EL-FLOW select) regulated the inlet flow of CO_2 and N_2 and measured the outlet flow of CO_2, from which an average value over the time has been calculated for each experiment. The functioning of the capture and release module is explained in Section 3.1, while the experimental set-up is sketched in the upper part of Scheme 2.

All the experiments have been performed at ambient temperature with a duration of 1.5 h and repeated at least twice to have reliable results. To have an optimal carbon capture and release, the variation of four parameters has been explored: current density (J = 25, 50, 75 and 100 mA/cm^2), CO_2 inlet flow rate (Q_{inlet} = 0, 5, 10 and 20 mL/min), pump flow rate (Q_{pump} = 1, 2.5 and 5 mL/min) and inlet CO_2/N_2 ratio (0%/0%, 100%/0%, 0%/100%, 50%/50%, 16%/84%).

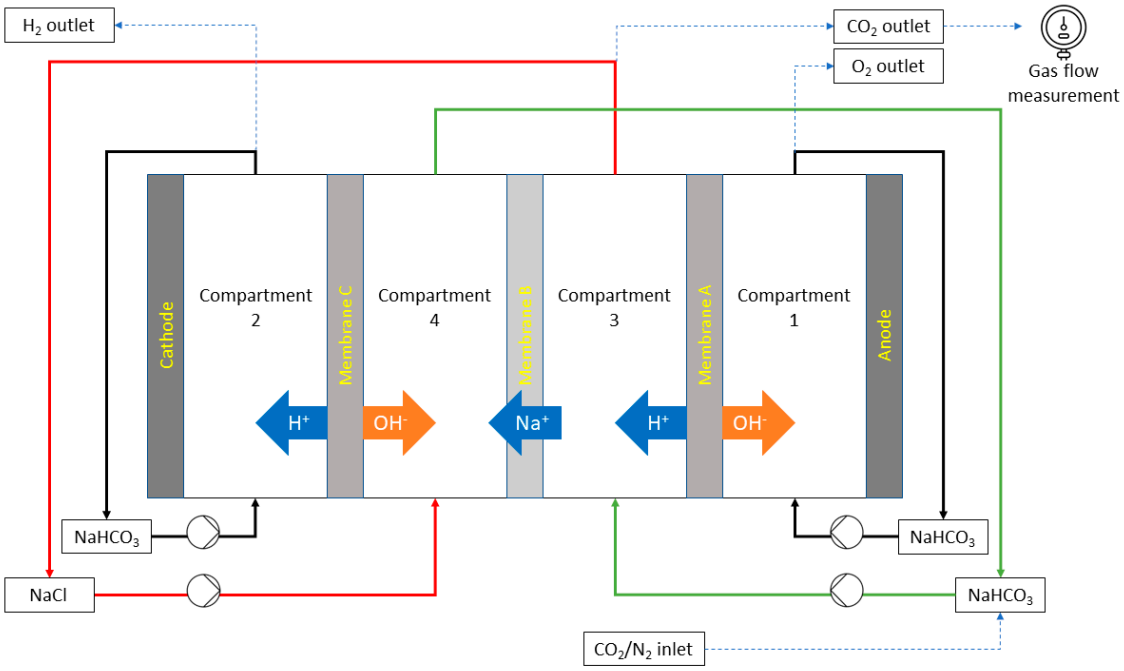

Scheme 1. Schematic representation of the capture and release module. Membrane A and C: bipolar membrane; Membrane B: cationic membrane.

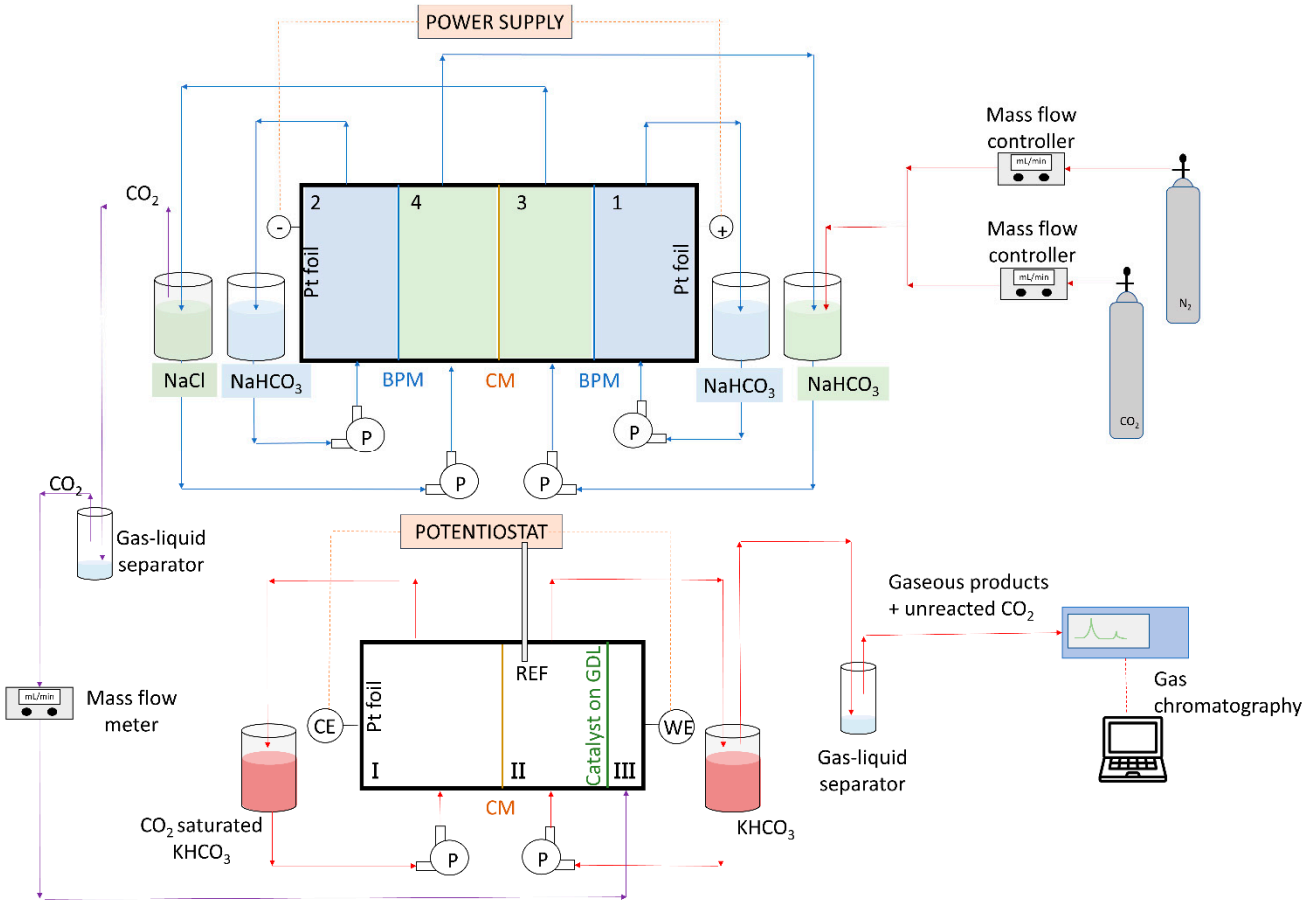

Scheme 2. Schematic representation of the coupling between the capture (upper reactor) and the conversion module (lower reactor). P: pump; CM: cationic membrane; BPM: bipolar membrane; CE: counter electrode; WE: working electrode; REF: reference electrode; GDL: gas diffusion layer.

2.2. Conversion Module

The conversion module has been used to convert the captured CO_2 into reusable products in a custom-made flow cell (ElectroCell, Micro Flow Cell). The CO_2 electrolysis has been carried out through chronoamperometry at an applied potential of −1.2 V vs. reversible hydrogen electrode (RHE) with a CHInstruments CHI760D electrochemical workstation. Eighty-five percent of the series resistance has been compensated by the instrument (iR-compensation). As illustrated in Scheme 2, a platinum foil has been employed as the counter electrode, a mini Ag/AgCl electrode (1 mm, leak-free LF-1) as the reference, and a catalyst coated carbon paper (GDL; SIGRACET 28BC, SGL Technologies) as the working electrode. The catalyst consisted of microwave-synthesized ZnO nanoparticles, as reported in our previous work [15]. An electrode with a geometric area of 1.5 cm^2 and a catalyst loading of 2.3 mg/cm^2 has been used [16]. The optimization of the conversion module has been carried out previously [15,16].

The anodic side included chamber I with the counter electrode, while the cathodic side consisted of chambers II and III with the reference and working electrodes. A proton exchange membrane (Nafion™ Membrane N117, Sigma-Aldrich) separated the chambers I and II, and the working electrode separated the chambers II and III. An aqueous 2 M $KHCO_3$ electrolyte was circulated through chambers I and II at a flow rate of 1.5 mL/min from an external reservoir. Before reaching chamber I, the electrolyte was saturated with a CO_2 flow at 10 mL/min from an external cylinder. Instead, the electrolyte in chamber II was not saturated by external CO_2. The CO_2 released from the capture module was the only CO_2 source for the cathodic side and entered in chamber III passing through the GDL and diffusing in the electrolyte in chamber II. The output gas stream from chamber II was separated from the liquid and analysed by a micro gas chromatograph (μGC, Fusion®, INFICON, Kawasaki City, Japan) equipped with two modules, one with a 10-m Rt-Molsieve 5A column and the other with an 8-m Rt-QBond column, both employing a microthermal conductivity detector (micro-TCD). The liquid products of circulating electrolyte in chamber II have been analyzed at the end of the measurement using a high-performance liquid chromatograph (multi modular Shimatzu HPLC). The separation is performed using a ReproGel H+ (300 × 8 mm) column using 9.0 mM H_2SO_4 (flow rate of 1.0 mL/min) as the mobile phase. The detector is a UV–Vis detector set at 210 nm.

The tests with the two coupled modules (capture and conversion) lasted 1.5 h and were performed at ambient conditions, employing gas stream input with CO_2/N_2 ratio equal to 50%/50% and 16%/84%, representative of a flue gas [17]. Before connecting the two modules, the capture one was let working for 2 h in order to assure that all the atmospheric gases have been removed from the gas line and a steady flow of CO_2 has been provided as input of the conversion module.

3. Results and Discussion

3.1. CO_2 Capture and Release

The capture and the release of CO_2 is performed by an electrochemical cell composed of four chambers, depicted in Scheme 1. In this system, the CO_2 recovery is performed by acidification of the sorbent solution, namely $NaHCO_3$. Cationic and bipolar membranes are arranged as shown in Scheme 1, since it is necessary to provide protons to the sorbent solution and to withdraw alkaline metal ions from it. Electrodialysis is the process to perform this exchange, allowing the release of gaseous CO_2 (outlet gas in Scheme 1), according to the following reactions:

$$CO_3^{2-} + H^+ \rightarrow HCO_3^- \quad (1)$$

$$HCO_3^- + H^+ \rightarrow H_2CO_3 \quad (2)$$

$$H_2CO_3 \rightarrow H_2O + CO_2 \quad (3)$$

Therefore, protons are provided to the feed compartment (compartment 3 in Scheme 1) by the bipolar membrane placed on the anode side of the cell (membrane A), while Na^+ ions cross the cationic membrane B reaching the alkali regeneration compartment (compartment 4) where NaCl is used as electrolyte. Here, hydroxyl ions are delivered by the bipolar membrane on cathode side (membrane C), consequently forming NaOH. The latter is then turned back into $NaHCO_3$ by the CO_2 present in the inlet flue gas, according to the Reaction 4, and driven again to the feed compartment; hence the process can restart.

$$NaOH + CO_2 \rightarrow NaHCO_3 \quad (4)$$

It is worth noticing that, in addition to the release of gaseous CO_2, there is also production of O_2 in the anodic (compartment 1) chamber and H_2 in the cathodic (compartment 2) chamber, due to water electrolysis. The hydrogen can be brought at the final outlet of the electrochemical reactor responsible for the reduction of carbon dioxide and added to syngas as final product.

Different tests were carried out to optimize the electrochemical capture and release cell, by changing the pump flow rate, the inlet gas flow rate, and the applied current density.

Figure 1 reports the voltage and the gas outlet flows (Q_{outlet}) trend for a typical experiment carried out at 100 mA/cm^2 with an inlet flow composed by 100% CO_2 at 20 mL/min. The voltage was stable between 12 V and 13 V for the entire 1.5 h-experiment. In the CO_2 flow, released from compartment 3, some traces of hydrogen and oxygen have been detected, probably due to the not perfect isolation among the compartments.

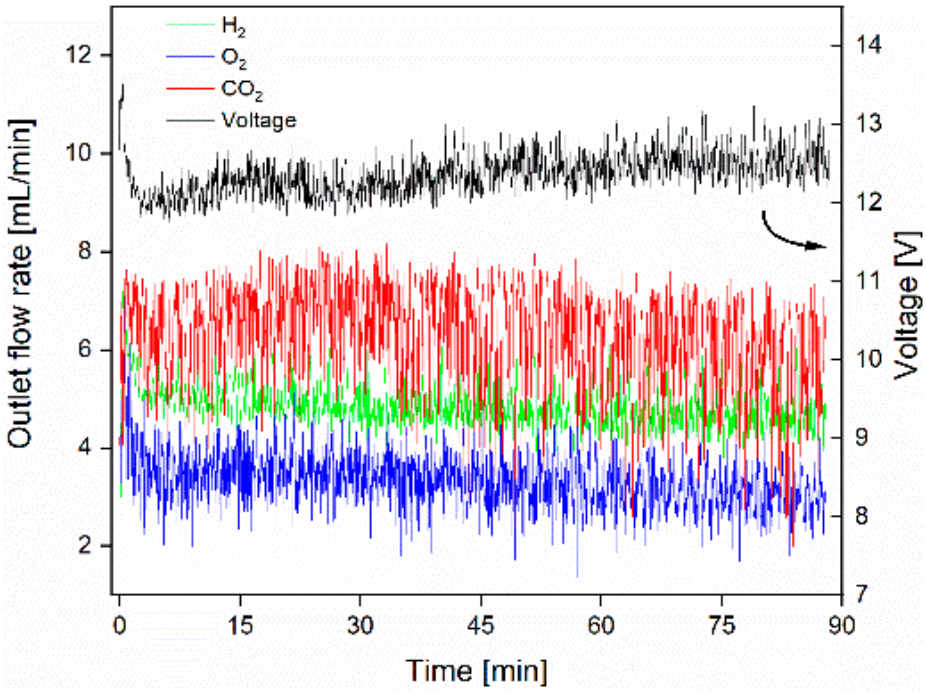

Figure 1. CO_2, O_2 and H_2 outlet flows (left axis) and measured voltage (right axis) in a typical experiment carried out with the capture and release unit (experimental conditions: J = 100 mA/cm^2, Q_{inlet} = 20 mL/min, Q_{pump} = 1 mL/min, CO_2/N_2 ratio = 100%/0%).

The effect of the variation of the current applied at the electrodes of the electrochemical cell on the release of CO_2 has been explored first. This is pointed out in Figure 2a,b. During the course of the experiments, stable voltages were measured, independently of the applied current density. As expected, a lower current brings a smaller voltage (12.5 V for 100 mA/cm^2 and 7 V for 25 mA/cm^2). Accordingly, the number of electrons involved in the reactions decreases, so that the production of carbon dioxide drops; likewise, the

outlet. In particular, the average outlet flow for J = 100 mA/cm^2 is almost doubled with respect to the value obtained at 75 mA/cm^2. This is coherent with the CO_2 recovery rate from carbonate calculated by Iizuka [18], which is proportional to the current applied at the electrodes. However, it is important to highlight that diminishing the voltage means to reduce the energy consumption of the capture system. This implies that, according to the needs of the conversion module that will get the carbon dioxide flow as an inlet, a proper trade-off between the current density and outlet flow is sometimes needed.

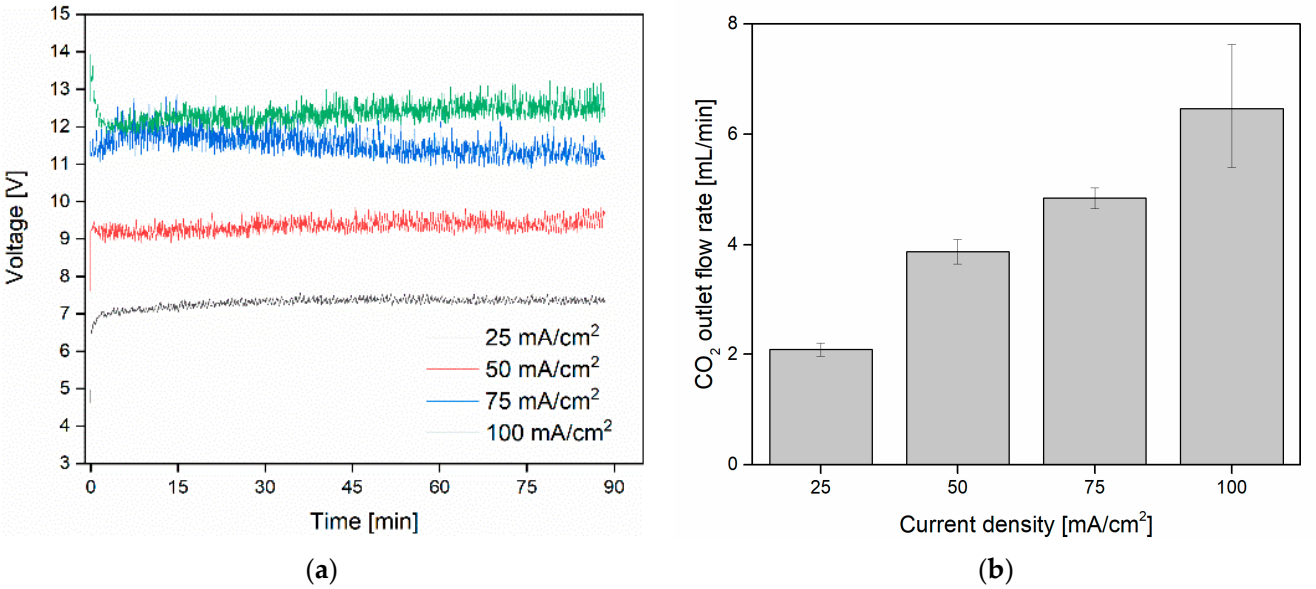

Figure 2. (**a**) Measured voltages for different applied current densities (experimental conditions: Q_{inlet} = 20 mL/min, Q_{pump} = 1 mL/min, CO_2/N_2 ratio = 100%/0%). (**b**) Average CO_2 flow for different applied current densities with the same experimental conditions.

The second parameter that has been optimized is the electrolyte flow rate, controlled by the peristaltic pump. The pump must make the sorbent solution and the electrolyte recirculate through the cell and the tanks, ensuring the regeneration of the bicarbonate, and therefore the perpetuation of the reactions. The optimization of this parameter is important since it controls the turbulence of the motion of the reactants, therefore changing the reaction rate inside the reactor. Figure 3 shows how the flow rate of reactants affects the average Q_{outlet} for CO_2. Q_{pump} = 1 mL/min is the best solution since it provides the highest average CO_2 outlet. Probably, the optimal pump flow rate, thus the recirculation of the reactants, is linked to the number of electrons provided at the electrodes, and therefore the current, as already observed in [19,20].

Since at this point a capture device was being implemented, one of the most important aspects is the percentage of CO_2 released with respect the amount of CO_2 bubbled in the solution. Figure 4 reports the average outlet CO_2 flow for different inlet gas flow rates. Considering Q_{inlet} = 10 mL/min and 5 mL/min, the percentage of carbon dioxide captured and released is larger (45% and 91% respectively) with respect to the case of Q_{inlet} = 20 mL/min (32%). It is important to take into account that part of the CO_2 released from the capture device in 1.5 h arises from the initial $NaHCO_3$ present in the electrochemical reactor, as shown in Figure 4 for Q_{inlet} = 0 mL/min. Once the initial $NaHCO_3$ is completely consumed, the outlet flow will be produced only by the acidification of carbonate regenerated by the bubbling carbon dioxide [18]. However, it has to be highlighted that this device has been designed expressly for the coupling with the conversion module. Since, overall, the outlet flow of CO_2 captured with Q_{inlet} = 20 mL/min is the largest one, this will make the performance of the whole capture/conversion system higher. For this reason, the optimized Q_{inlet} will be selected to maximize the performance of the whole coupled system, i.e., 20 mL/min.

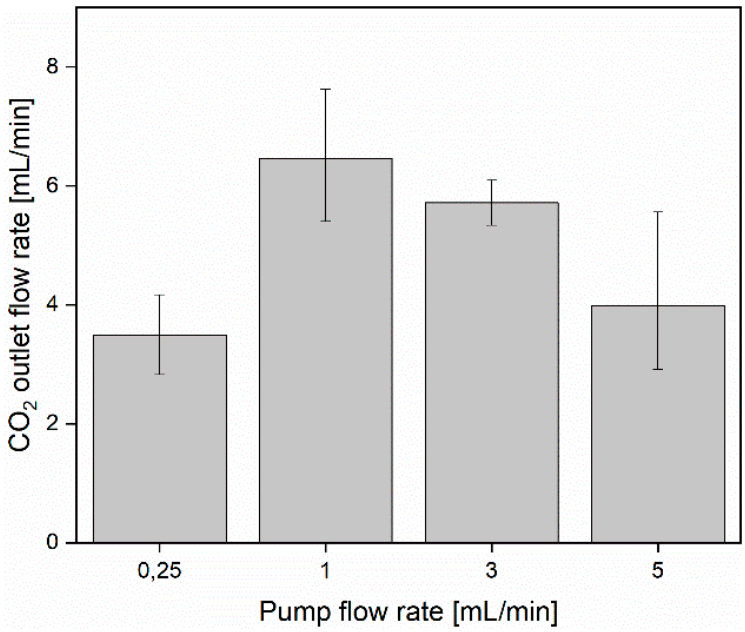

Figure 3. Average CO_2 flow for different pump flow rates (experimental conditions: Q_{inlet} = 20 mL/min, J = 100 mA/cm^2, CO_2/N_2 ratio = 100%/0%).

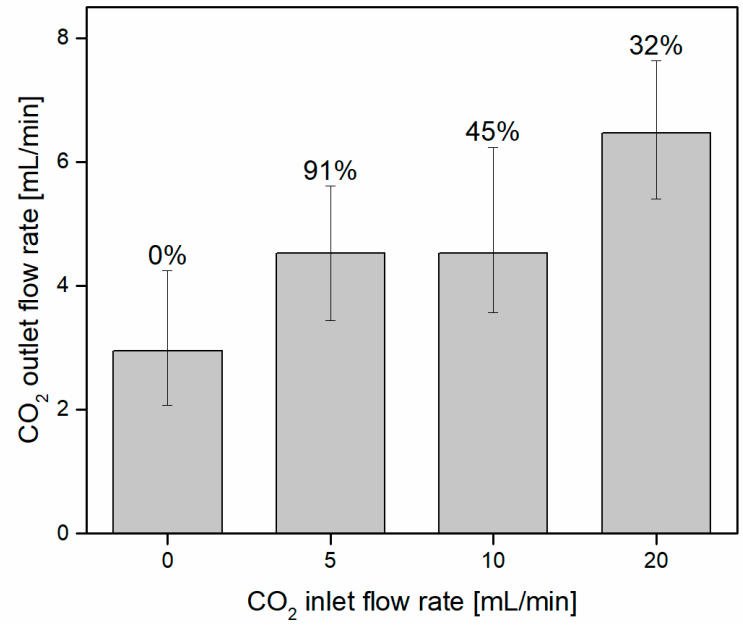

Figure 4. Average CO_2 flow for different pure CO_2 inlet flow rates (experimental conditions: J = 100 mA/cm^2, Q_{pump} = 1 mL/min, CO_2/N_2 ratio = 100%/0%). The values on top of the columns represent the percentage of CO_2 captured with respect to that provided as input.

So far, the parameters have been changed to optimize the outlet flow, but the real capture of carbon dioxide from flue gas has never been simulated. In this regard, the outlet was studied dependently on the percentage of the composition of the inlet gas. In order to simulate a flue gas, a mixture of CO_2 and N_2 was being bubbled through. Figure 5 points out that the presence of nitrogen in the inlet gas does not influence the outlet, which is almost the same for the case in which no bubbling gas is present. Indeed, the presence of an additional bubbling flow, such as nitrogen, could even help in the regeneration of the bicarbonate, increasing the turbulent motion in the tank. In addition, Figure 5 provides the

result with a flue gas as the inlet, in which the CO_2 component is kept at 20 mL/min. It can be observed that the final average CO_2 outlet flow, with 50% and 84% of nitrogen as the inlet, does not depart too much from the case of pure CO_2.

Figure 6 considers the findings mentioned so far and highlights the dependence of the CO_2 outlet flow rate on both CO_2 inlet flow rate and pump flow rate (the current density is not taken into account here since the output flow rate is directly proportional to J). The surface has been constructed employing Matlab, implementing a fit through a piecewise cubic interpolation of the data obtained during the tests. It can be noticed that for large pump flow rates the CO_2 outlet flow decreases. Moreover, having a higher CO_2 inlet helps to have a larger outlet. In order to maximize the gas outlet and perform the coupling with the conversion module, looking at Figure 6, the best condition seems to be described by the area where the parameters Q_{inlet} and Q_{pump} are about 20 mL/min and 1 mL/min, respectively. For this reason, the following set of parameters have been employed for the subsequent part of the work: Q_{inlet} = 20 mL/min, Q_{pump} = 1 mL/min and J = 100 mA/cm^2.

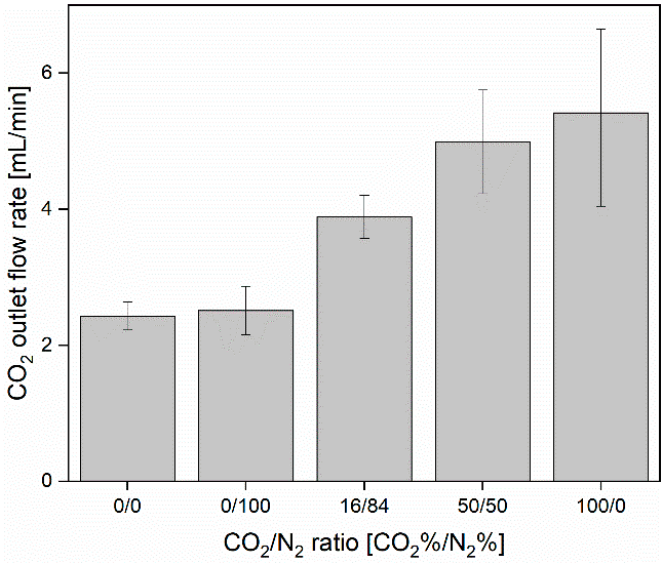

Figure 5. Average CO_2 flow for different compositions of inlet gas (experimental conditions: Q_{inlet} = 20 mL/min, Q_{pump} = 5 mL/min, J = 100 mA/cm^2).

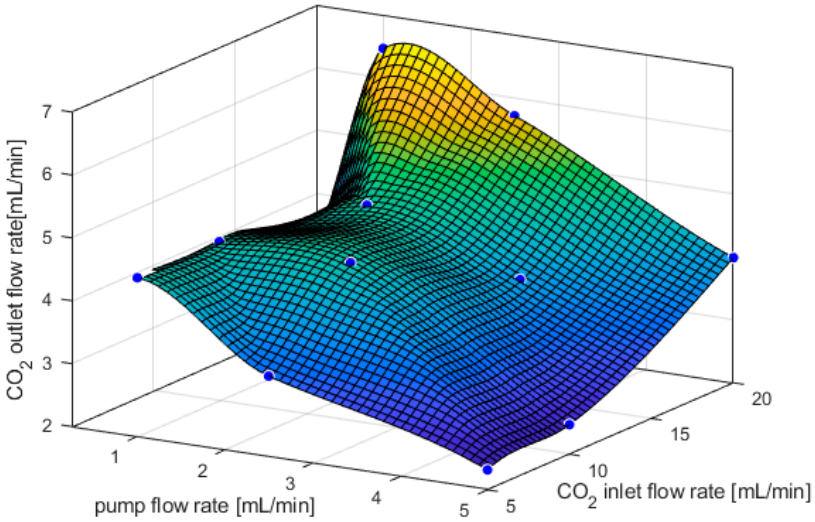

Figure 6. Interpolating fit of experimental CO_2 outlet results obtained at J = 100 mA/cm^2 for different CO_2 inlet and pump flow rates. The blue points are the experimental data.

A stability test of the capture/release system of 8 h has been performed with the optimized parameters employing pure CO_2 flow as inlet. Three parameters have been monitored during the whole experiment: the outlet gas flow, the voltage, and the outlet gas composition. Figure 7 reports the trend of these three parameters and shows how after around 2 h the voltage and the outlet gas reach a stable value, around 12 V and 5 mL/min respectively. Probably, this is the time necessary for the hydraulic system to completely mix the sorbent and the electrolyte solutions between the tanks that feed compartments 3 and 4 (see Scheme 1). The composition of the outlet gas has been monitored during the entire test. After 1 h, the output gas phase was composed by 98% of CO_2 and it remained stable for the rest of the experiment. Therefore, this stability test shows how the capture module is able to provide a constant pure amount of carbon dioxide for a long time interval. Similar purities of the outlet stream have been obtained in analogous experiments performed with a simulated flue gas (CO_2/N_2 mixtures of 50%/50% and 16%/84%) as the inlet.

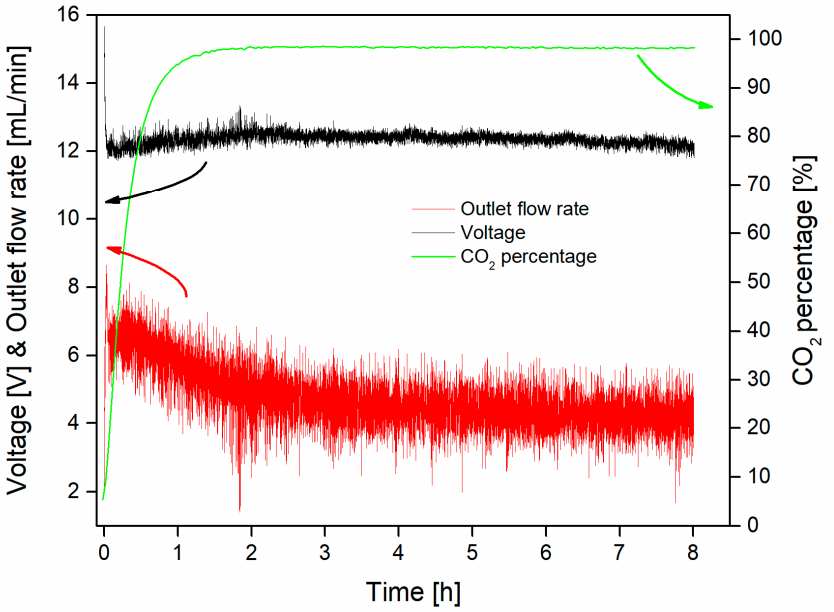

Figure 7. Measured voltage (left axis), CO_2 outlet flow rate, and purity of CO_2 in the outlet gas (right axis) during the stability test of eight hours (experimental conditions: Q_{inlet} = 20 mL/min, Q_{pump} = 1 mL/min, J = 100 mA/cm^2, CO_2/N_2 ratio = 100%/0%).

Considering the results obtained in the stability test, the energy spent by the system per unit of carbon dioxide recovered from the bicarbonate is 42.5 MJ/kgCO_2. This result makes clear that this particular capture system has to be further optimized. In fact, the comparison with the similar system introduced by Nagasawa [13], characterized by a minimum recovery power requirement of 2.1 MJ/kgCO_2, and with a typical amine-based process (3–4 MJ/kgCO_2), shows how this precursory system has the possibility to be proficient, avoiding the use of toxic agents like amines. One possibility would be a stack composed by two of this system in order to decrease the ohmic losses. In addition, two different nanostructured electrocatalysts could replace the platinum foil at the anode and the cathode, increasing the energy efficiency.

3.2. Capture–Conversion Coupling

At this point, the capture system has been optimized and its outlet has been connected to the CO_2 reduction reaction (CO_2RR) module, as shown in the Scheme 2.

The CO_2 released by the capture module enters the chamber III, where it can diffuse through the GDL and reach the ZnO catalyst/electrolyte interface in chamber II. For a cathodic applied potential of −1.2 V (whole cell potential of 3.2 V), the CO_2 can be reduced to CO (Equation (5)) and HCOOH or $HCOO^-$ (Equation (6)). Hydrogen can also be

produced (Equation (7)). The ZnO catalyst is more selective towards CO, and thus the formic acid production is scarce [15]. The gaseous products are CO and H_2, which are the components of syngas.

$$CO_2 + H_2O + 2e^- \rightarrow CO + 2OH^- \quad (5)$$

$$CO_2 + H_2O + 2e^- \rightarrow HCOO^- + OH^- \quad (6)$$

$$2H_2O + 2e^- \rightarrow H_2 + 2OH^- \quad (7)$$

In order to test the catalyst performance under optimal conditions, a preliminary experiment has been conducted employing a CO_2 flux of 25 mL/min from an external cylinder as the CO_2 source for the cathodic side. A current density of 40.9 mA/cm^2 and faradaic efficiencies of 69% for CO, 27% for H_2, and 4% for HCOOH have been obtained. Then the CO_2 gas flow has been decreased to 3 mL/min, to mimic the release rate of CO_2 from the capture module. The current density maintains a similar value of 43.6 mA/cm^2, while the selectivities exhibit a notable difference, namely 56% for CO, 40% for H_2 and 4% for HCOOH. This outcome indicates that the CO_2RR performance is significantly influenced by the CO_2 flow rate; smaller values can decelerate the mass diffusion process and induce an increase of hydrogen evolution.

Then, two different tests with CO_2/N_2 gas mixtures equal to 50%/50% and 16%/84% were carried out. The capture module worked at the optimized conditions described in the previous section. The 50%/50% gas mixture releases an outlet gas flux of 3 mL/min. It is lower than that obtained in the previous tests (see Figure 5), probably due to the coupling with the conversion module, which introduces an obstacle to the gas flux, raising the pressure and therefore reducing the flow rate. During the test, the conversion module showed stable selectivity and current density, as displayed in Figure 8. An average current density of 35.9 mA/cm^2 and faradaic efficiencies of 56% for CO, 41% for H_2, and 3% for HCOOH have been achieved. These results are in line with those obtained with a CO_2 flux of 3 mL/min from an external cylinder. It is clear that not all the provided CO_2 can react, and around 14.8% of the total amount is converted into CO and HCOOH.

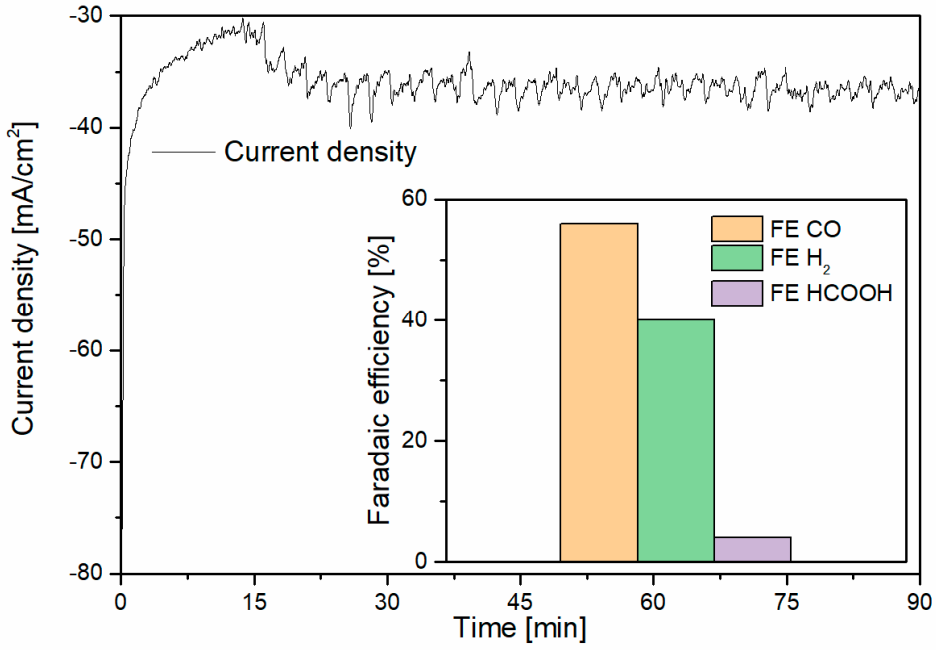

Figure 8. Conversion module results with an initial 50%/50% gas stream; average current density during the measure and (inset) faradaic efficiencies of the reaction products (FE = faradaic efficiency).

For the second test, the CO_2/N_2 16%/84% gas stream has been used. The outlet flow rate from the capture module was 1.5 mL/min, smaller if compared to the one obtained without the conversion module, due to the same reason described above. As shown in Figure 9, the current density is 39.6 mA/cm^2 and the faradaic efficiency is 37% for CO, 59% for H_2, and 4% for HCOOH. The selectivity towards CO_2RR products is further decreased, due to the lower CO_2 flow rate at the cathodic side of the flow cell, while the percentage of reacted CO_2 rises up to 22.6% during this test.

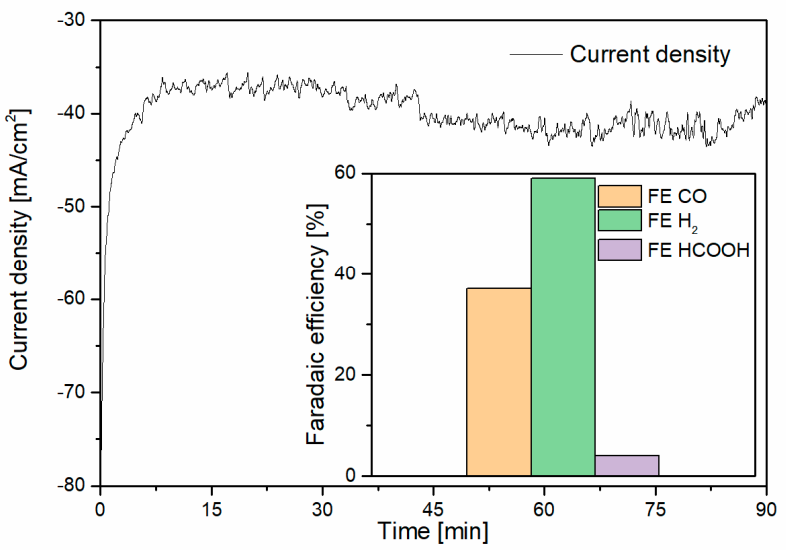

Figure 9. Conversion module results with an initial 16%/84% gas stream; average current density during the measure and (inset) faradaic efficiencies of the reaction products (FE = faradaic efficiency).

By comparing the results of the two tests, it can be observed that with decreased CO_2 percentage in the initial gas stream, the absorption module has reduced its released gas flux. This induces a CO_2 mass diffusion limitation at the conversion module as described before. Despite this issue, which reserves additional investigations aimed at optimizing the coupling between the modules, the electrochemical platform demonstrated its ability to separate CO_2 from simulated flue gas mixtures and convert it into value added products. Syngas with CO:H_2 ratios from 1.4 to 0.6 has been produced at good current densities of 35–40 mA/cm^2. The composition of the obtained syngas is similar to the one commonly used for the synthesis of ethanol [21]. This system can be employed for the capture of harmful emissions and their transformation into useful resources in both industrial and civil scenarios. Moreover, the use of green chemicals such as sodium chloride and sodium/potassium bicarbonates makes it particularly appealing in the framework of sustainable CCU.

4. Conclusions

For the first time, a completely electrochemical platform able to capture CO_2 from flue gas and convert it in syngas has been successfully implemented.

The platform consists of the coupling of two different modules (capture and conversion) that were, at first, separately optimized. The CO_2 capture is performed by electrolysis of a carbonate solution inside an electrochemical flow cell. In order to have the highest CO_2 outlet flow rate, the set-up of the electrochemical reactor was optimized through experiments of 1.5 h in terms of flow rate of the flue gas inlet (20 mL/min), simulated by the CO_2–N_2 mixture, flow rate of the recirculating sorbent solution (1 mL/min), and current density (100 mA/cm^2). In addition, it was shown that the presence of nitrogen at the inlet does not affect the outlet of the reactor. A stability test that lasted eight hours showed that the system can capture the CO_2 and provide at the outlet a stable and very pure (>98%) flux (5 mL/min) during the whole interval.

The second component is another electrochemical flow cell, responsible for the conversion of the carbon dioxide released by the capture module in a CO–H_2 mixture. The reduction of the CO_2 was performed by a catalyst composed of ZnO nanoparticles. Stable high current densities up to 40 mA/cm^2 have been obtained from this module, producing syngas with various CO:H_2 ratios.

This work shows how it is possible to develop an electrochemical device, which can be easily integrated, for CO_2 capture and conversion. Given its intrinsic characteristic, it is possible to supply the whole system by renewable energy, in order to avoid additional carbon dioxide emissions, and to further exploit the concept of carbon neutral process. At the same time, the energy consumption must be reduced to increase the efficiency in terms of captured/converted CO_2 with respect to the energy required, and this could be done by further optimization of the device.

Author Contributions: Conceptualization, S.B. and A.S.; methodology, A.M., A.P., N.B.D.M., M.A.F., J.Z. and A.S.; validation, A.M., A.P. and N.B.D.M.; investigation, A.M., A.P. and N.B.D.M.; resources, A.C and C.F.P.; writing—original draft preparation, A.M. and N.B.D.M.; writing—review and editing, A.M., A.P., N.B.D.M., S.B., J.Z., A.C. and A.S.; supervision, A.S.; funding acquisition, C.F.P. All authors have read and agreed to the published version of the manuscript.

Funding: This research received no external funding.

Data Availability Statement: The data presented in this study is available on request from the corresponding author.

Conflicts of Interest: The authors declare no conflict of interest.

References

1. Gibbins, J.; Chalmers, H. Carbon capture and storage. *Energy Policy* **2008**, *36*, 4317–4322. [CrossRef]
2. Pardal, T.; Messias, S.; Sousa, M.; Machado, A.S.R.; Rangel, C.M.; Nunes, D.; Pinto, J.V.; Martins, R.; da Ponte, M.N. Syngas production by electrochemical CO_2 reduction in an ionic liquid based-electrolyte. *J. CO_2 Util.* **2017**, *18*, 62–72. [CrossRef]
3. Jung, J.; Jeong, Y.S.; Lim, Y.; Lee, C.S.; Han, C. Advanced CO_2 Capture Process Using MEA Scrubbing: Configuration of a Split Flow and Phase Separation Heat Exchanger. *Energy Proc.* **2013**, *37*, 1778–1784. [CrossRef]
4. Liu, M.; Asgar, H.; Seifert, S.; Gadikota, G. Novel aqueous amine looping approach for the direct capture, conversion and storage of CO_2 to produce magnesium carbonate. *Sustain. Energy Fuels* **2020**, *4*, 1265–1275. [CrossRef]
5. Liu, M.; Gadikota, G. Integrated CO_2 Capture, Conversion, and Storage to Produce Calcium Carbonate Using an Amine Looping Strategy. *Energy Fuels* **2019**, *33*, 1722–1733. [CrossRef]
6. Bhattacharya, M.; Sebghati, S.; VanderLinden, R.T.; Saouma, C.T. Toward Combined Carbon Capture and Recycling: Addition of an Amine Alters Product Selectivity from CO to Formic Acid in Manganese Catalyzed Reduction of CO_2. *J. Am. Chem. Soc.* **2020**, *142*, 17589–17597. [CrossRef]
7. Lombardo, L.; Ko, Y.; Zhao, K.; Yang, H.; Züttel, A. Direct CO_2 Capture and Reduction to High-End Chemicals with Tetraalkylammonium Borohydrides. *Angew. Chem. Int. Edit.* **2021**, *60*, 9580–9589. [CrossRef]
8. Wilkes, J.S. A short history of ionic liquids—from molten salts to neoteric solvents. *Green Chem.* **2002**, *4*, 73–80. [CrossRef]
9. Kosaka, F.; Liu, Y.; Chen, S.-Y.; Mochizuki, T.; Takagi, H.; Urakawa, A.; Kuramoto, K. Enhanced Activity of Integrated CO_2 Capture and Reduction to CH_4 under Pressurized Conditions toward Atmospheric CO_2 Utilization. *ACS Sustain. Chem. Eng.* **2021**, *9*, 3452–3463. [CrossRef]
10. Duyar, M.S.; Treviño, M.A.A.; Farrauto, R.J. Dual function materials for CO_2 capture and conversion using renewable H_2. *Appl. Catal. B Environ.* **2015**, *168–169*, 370–376. [CrossRef]
11. Ampelli, C.; Genovese, C.; Errahali, M.; Gatti, G.; Marchese, L.; Perathoner, S.; Centi, G. CO_2 capture and reduction to liquid fuels in a novel electrochemical setup by using metal-doped conjugated microporous polymers. *J. Appl. Electrochem.* **2015**, *45*, 701–713. [CrossRef]
12. Song, C.; Pan, W. Tri-reforming of methane: A novel concept for catalytic production of industrially useful synthesis gas with desired H_2/CO ratios. *Catal. Today* **2004**, *98*, 463–484. [CrossRef]
13. Nagasawa, H.; Yamasaki, A.; Iizuka, A.; Kumagai, K.; Yanagisawa, Y. A new recovery process of carbon dioxide from alkaline carbonate solution via electrodialysis. *AIChE J.* **2009**, *55*, 3286–3293. [CrossRef]
14. Zeng, J.; Bejtka, K.; Di Martino, G.; Sacco, A.; Castellino, M.; Re Fiorentin, M.; Risplendi, F.; Farkhondehfal, M.A.; Hernández, S.; Cicero, G.; et al. Microwave-Assisted Synthesis of Copper-Based Electrocatalysts for Converting Carbon Dioxide to Tunable Syngas. *ChemElectroChem* **2020**, *7*, 229–238. [CrossRef]
15. Zeng, J.; Rino, T.; Bejtka, K.; Castellino, M.; Sacco, A.; Farkhondehfal, M.A.; Chiodoni, A.; Drago, F.; Pirri, C.F. Coupled Copper–Zinc Catalysts for Electrochemical Reduction of Carbon Dioxide. *ChemSusChem* **2020**, *13*, 4128–4139. [CrossRef]

16. Lourenço, M.A.O.; Zeng, J.; Jagdale, P.; Castellino, M.; Sacco, A.; Farkhondehfal, M.A.; Pirri, C.F. Biochar/Zinc Oxide Composites as Effective Catalysts for Electrochemical CO_2 Reduction. *ACS Sustain. Chem. Eng.* **2021**, *9*, 5445–5453. [CrossRef]
17. Jin, S.; Wu, M.; Gordon, R.G.; Aziz, M.J.; Kwabi, D.G. pH swing cycle for CO_2 capture electrochemically driven through proton-coupled electron transfer. *Energy Environ. Sci.* **2020**, *13*, 3706–3722. [CrossRef]
18. Iizuka, A.; Hashimoto, K.; Nagasawa, H.; Kumagai, K.; Yanagisawa, Y.; Yamasaki, A. Carbon dioxide recovery from carbonate solutions using bipolar membrane electrodialysis. *Sep. Purif. Technol.* **2012**, *101*, 49–59. [CrossRef]
19. Feng, S.; Yang, G.; Zheng, D.; Wang, L.; Wang, W.; Wu, Z.; Liu, F. A dual-electrolyte aluminum/air microfluidic cell with enhanced voltage, power density and electrolyte utilization via a novel composite membrane. *J. Power Sources* **2020**, *478*, 228960. [CrossRef]
20. Ma, X.; Zhang, H.; Sun, C.; Zou, Y.; Zhang, T. An optimal strategy of electrolyte flow rate for vanadium redox flow battery. *J. Power Sources* **2012**, *203*, 153–158. [CrossRef]
21. Chae, H.J.; Kim, J.-H.; Lee, S.C.; Kim, H.-S.; Jo, S.B.; Ryu, J.-H.; Kim, T.Y.; Lee, C.H.; Kim, S.J.; Kang, S.-H.; et al. Catalytic Technologies for CO Hydrogenation for the Production of Light Hydrocarbons and Middle Distillates. *Catalysts* **2020**, *10*, 99. [CrossRef]